Impact of seismic retrofit and presence of *terra cotta* masonry walls on the dynamic properties of a hospital building in Montréal, Canada

A. Asgarian & G. McClure
Civil Engineering and Applied Mechanics, McGill University

15 WCEE
LISBOA 2012

SUMMARY:
Unreinforced masonry (URM) infill walls are widely used in structures. Since they are generally considered as non-structural components, their structural effects are often ignored. However, infill walls interact with their surrounding frame during earthquakes and influence the dynamic properties of the building, which can lead to some unaccounted for and undesired earthquake-induced damages. This is of importance when performing seismic assessment of post-critical buildings such as hospitals. To illustrate the significant structural contribution of infill walls, two eleven-storey buildings have been selected which are two wings of a hospital. A detailed elastic finite element model was created where the infill walls have been modeled. In parallel, *in situ* ambient vibration measurements were done in both buildings and their dominant dynamic properties were extracted to calibrate the numerical models. Subjecting the calibrated model to a set of ground accelerograms, inter-storey drift curves and floor response spectra (FRS) were developed. The effects of seismic retrofit and presence of infill walls on the dynamic properties of the building and also on the performance of their NSCs were addressed by comparing the results of different models. Finally, a detailed study of the NSC's seismic behaviour was done using FRS and inter-storey drift curves.

Keywords: Earthquake Engineering, Unreinforced Infill Walls, Non Structural Components, Floor Response Spectra.

1. INTRODUCTION

In general, building components can be categorized into two groups: structural components and non-structural components (NSCs). NSCs can be sub-categorized into three types: architectural, building services, and building contents (CSA 2006). Unreinforced masonry (URM) infill walls are a common example of architectural components which are widely used for low- and medium-rise buildings all over the world in regions of low to high seismicity. In several "pre-code" hospital buildings constructed before the 1970s, *terra cotta* masonry blocks have been used extensively both as infill walls and partitions (Figure 1.1). Although infill walls are considered as NSCs, yet during the earthquake, they tend to interact with the surrounding frame which results in an increase in the lateral stiffness and strength of the structure, and in turn influences the dynamic response of the building. Of course, as they get damaged in strong earthquakes, their stiffness is degrading and they either become locally detached from the frame or they simply collapse. Thus, ignoring the frame-wall interaction is not always on the conservative side and it may lead to erroneous estimation of the lateral stiffness, strength, and ductility of the structure. In addition, the presence of URM infill walls can also cause some undesired behaviour such as brittle shear failure of reinforced concrete columns and short column phenomenon, over-strengthening of the upper stories of the structure, or induce a soft first storey and torsional effects due to in-plane irregularity. *In situ* vibration measurements and observations of past earthquake-induced damage clearly demonstrate the necessity of considering the effect of infill walls, particularly for post-critical buildings such as hospitals which have to remain functional after severe design-level seismic motions.

To illustrate the structural contribution of infill *terra cotta* walls, a detailed case study analysis has

been done on two eleven-storey wings (Blocks #7 and #8) of CHU Sainte-Justine, a paediatric research hospital located in Montréal, Canada. The two buildings are mostly identical in terms of floor plans, elevations and dimensions, and their lateral-load resisting structure is a reinforced concrete moment-resisting frame. The hospital campus was initially built in the late 1950s and expanded over the years: it now comprises 12 individual buildings identified on the schematic plan view of Figure 1.2. Block #7 was seismically retrofitted in 2008 by adding a full-height reinforced concrete shear wall at its free end and connecting the other end of the building to the adjacent Block #9 using structural anchor bars at each floor slab and along the height of interfacing columns. Block #8 was not retrofitted and has remained unattached to its adjacent building.

Figure 1.1. *Terra Cotta* infill masonry walls in CHU Sainte-Justine in Montréal (Asgarian 2010).
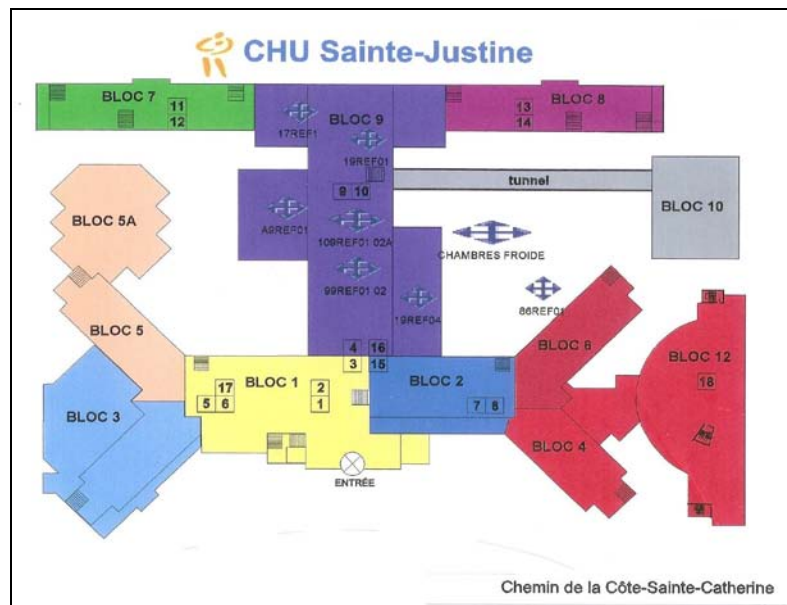
Figure 1.2. General plan layout of the hospital (Chartrand 2009).

2. SCOPE OF THE STUDY

The main goal of this study is to achieve better understanding of the effect of non structural wall components, in this case unreinforced *terra cotta* infill walls, on the dynamic behavior of buildings during strong ground motions. A secondary goal is to assess the impact of seismic rehabilitation and the presence of infill masonry walls on the seismic performance of NSCs and building contents. To meet these objectives, the research was divided into two phases:

- A numerical study: in which detailed linear elastic finite element analysis structural models of Blocks #7 and #8 have been generated where the infill unreinforced *terra cotta* walls are explicitly modelled using two different techniques, namely panel elements and simplified compression strut models.

- An experimental study: in which ambient vibration measurements (AVM) have been conducted in the same buildings. Then, the dominant dynamic properties of both buildings, including the lowest natural frequencies, corresponding mode shapes, and effective modal damping ratios, were extracted using operational modal analysis techniques.

The dynamic properties extracted from AVM results have then been utilized to calibrate and verify the finite element models of the two buildings. Lastly, the effects of seismic retrofit and infill walls on the dynamic properties of the buildings and also on the performance of their NSCs are assessed by comparing the different models and by developing floor response spectra (FRS) and inter-storey drift curves after subjecting the calibrated models to different ground accelerograms.

3. EXPERIMENTAL STUDY: *IN SITU* AMBIENT VIBRATION MEASUREMENTS (AVM)

For the purpose of verifying and calibrating the numerical models, ambient vibration measurements (AVT) were performed in the two selected buildings (Blocks #7 and #8) of CHU Sainte-Justine. The floor velocities induced by ambient excitations in both horizontal directions and along the vertical were recorded at several locations in each building to enable the identification of the main low frequency modes of vibration including both translational modes in the principal directions and the first torsional mode. Figure 3.1 illustrates the typical layout for AVM measurements.

Conducting the Singular Value Decomposition (SVD) on recorded data (Schott 2005), the singular value plots were extracted in which some of the peaks correspond to the natural frequencies of the structure. Data analysis has been done using two different operational modal analysis techniques, namely, Frequency Domain Decomposition-Peak Picking (FDD) and Enhanced Frequency Domain Decomposition-Peak Picking (EFDD) as implemented in the commercial software ARTeMIS Extractor[TM]. The dominant dynamic properties of both buildings including the lowest natural frequencies, corresponding mode shapes, and effective modal damping ratios have been extracted (Structural Vibration Solutions 2010). The first series of AVM tests was done in August and September 2010 in both buildings. Due to some discrepancies between AVM results and numerical results obtained with models of Block#7, another test series was conducted only in this block in July 2011 to clarify the source of inconsistency. The AVM results for both blocks are presented in Table 3.1 for the first three modes of vibration. Further explanations about the theoretical concepts and analytical details can be found in Asgarian (2012) and Gilles (2011).
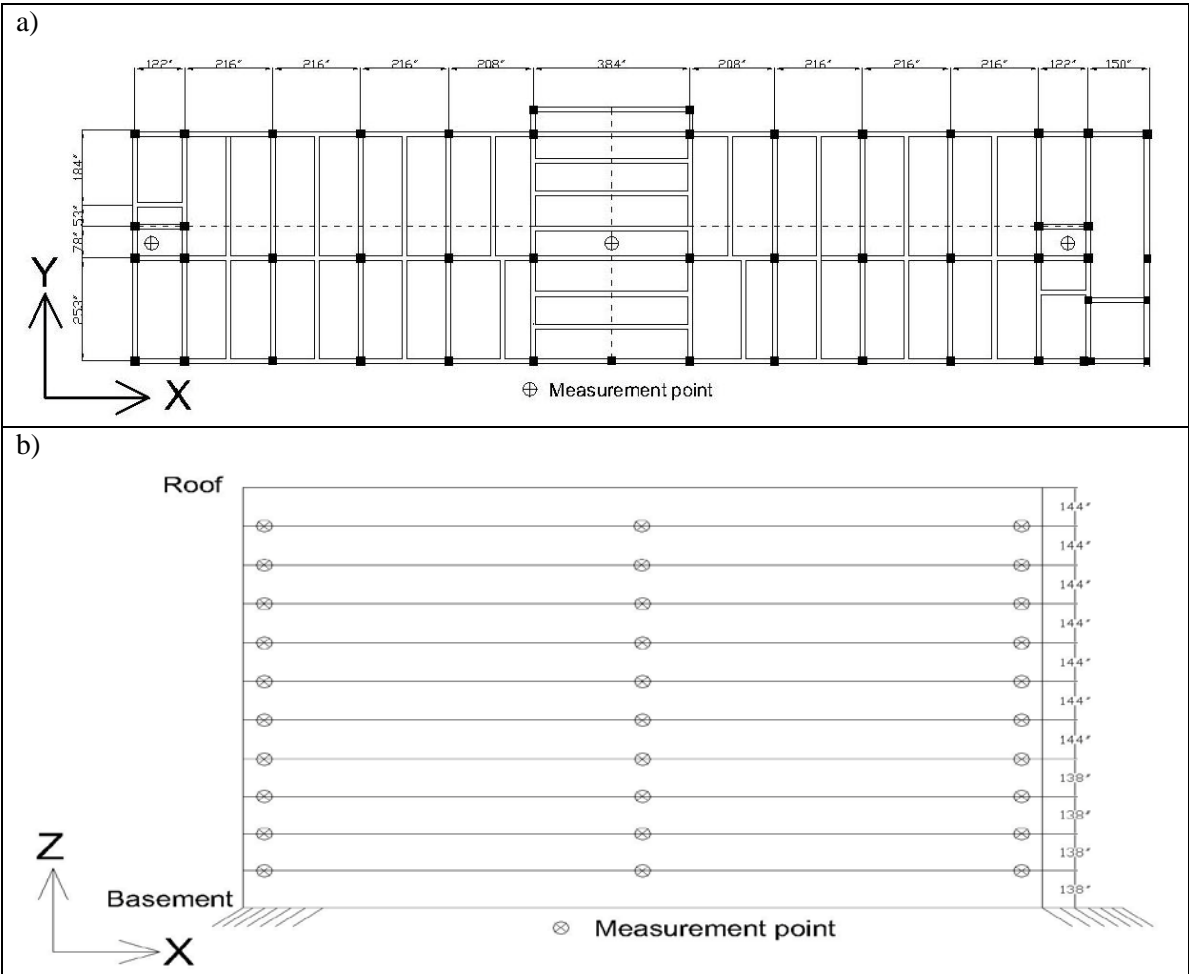
Figure 3.1. Distribution of measurement points: a) Horizontal plane; b) Vertical direction.

4. NUMERICAL STUDY

To study the effect of seismic retrofitting and masonry infill walls on the dynamic characteristics of the two buildings and also on seismic performance of their NSCs, several different linear elastic 3D finite element analysis models were generated in SAP2000 v.14.0.0 (Computers and Structures 2009), which can be divided in two groups: Bare-frame models excluding infill walls, and Full-frame models in which the infills have been added.

4.1. Bare-frame models

As the first step of the numerical study, the bare-frame models of both blocks were generated in which only the structural elements comprising beams, columns, concrete slabs, and concrete shear-wall (only for Block#7) are modelled and infill walls are excluded. However, to account for the self-weight (dead load) associated with the partitions and infill walls in the models, a dead load of 1 kPa has been distributed uniformly on all floor areas (except roof), as stipulated in the National Building Code of Canada NBC 2005 Division B-4.1.4.1.(3) (National Research Council of Canada 2005),

4.2. Full-frame models

To evaluate the effect of masonry infill walls on the dynamic properties of the building, the masonry infill walls have been added to the initial bare-frame models to develop the full-frame models. Previous studies on infill wall modeling can be generally divided into two groups of techniques: equivalent diagonal compression strut models and finite element models of wall panels.

4.2.1. *Equivalent diagonal compression struts*
Polyakov (1960) was the first to publish a study on the behaviour of infilled reinforced concrete frames subjected to racking load. Monotonic load testing of a number of large-scale frames indicated that the masonry infill and frame elements behave elastically until separation cracks developed between the infill and the frame perimeter except for small regions at the two diagonally opposite corners subjected to compression. Based on these observations, Polyakov suggested that the infilled frame system is equivalent to a braced frame with a compression diagonal strut replacing the infill wall (Figure 4.1-a). Holmes (1961) further developed this idea and proposed that the infill wall acts as an equivalent diagonal compression strut of the same thickness and elastic modulus as the infill with a width equal to one-third the diagonal length. Stafford Smith (1967) introduced the concept of "effective width" of the wall (instead of one-third the diagonal length) as the width of an equally stiff uniform strut, and he determined that the effective width is dependent on the wall's aspect ratio and the relative lateral stiffness of the frame columns and masonry infill. More recently, further studies have developed this concept of diagonal strut: see Mainstone and Station (1974), Hendry (1981), Durrani *et al.* (1994), Shing and Mehrabi (2002), FEMA-356 (FEMA and ASCE 2000), and El-Dakhakhni (2000 and 2003). Three of these approaches, namely those of Stafford Smith, Durrani and Luo, and FEMA-356 have been adopted in this study for the equivalent strut models. More details can be found in Asgarian (2012).

4.2.2. *Finite element models*
Taking advantage of advances in computational techniques and computer technology, it is relatively simple to use a more detailed modeling approach for masonry infill walls using finite elements. The main difficulty is to determine the characteristics of the interface between the masonry and the mortar, and that between the infill panel and its surrounding frame, and secondly defining the material properties that are representative of the composite material behaviour of the wall (Mohyeddin-Kermani *et al.* 2008). The approach adopted in this study to model the infills is to consider the *terra cotta* masonry as a homogeneous material representing the masonry block units and the mortar as a continuum, which is referred to as "a homogeneous isotropic continuum" in the literature (Figure 4.1-b). The walls are therefore modeled using plane stress panel elements with equivalent homogeneous elastic properties.
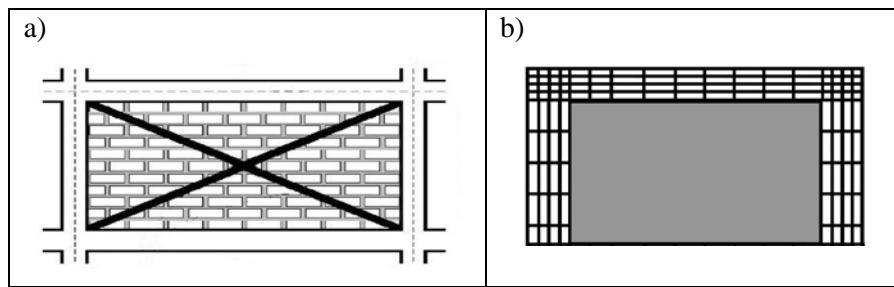
Figure 4.1. Masonry infill walls modeling: a) Diagonal compression struts; b) Continuum model (Panel element)

4.3. Calibration of numerical models using AVM results

Determining the appropriate material properties of the masonry infill is a difficult task. The smallest nominal value of the compressive strength recommended for *terra cotta* infill walls in masonry standards (ACI 530 2005) and handbook (Amrhein 1998) was selected as the starting assumption. Then, after completion of the initial frequency analysis, the results have been compared with those extracted from the AVM records and the initial material properties were replaced by those resulting in the best match between the first three natural frequencies of the continuum model and AVM results. These revised masonry properties were then applied to all the finite element models that included infill walls.

4.4. Time-history seismic analysis and development of FRS and inter-storey drift curves

The calibrated finite element models were subjected to a series of horizontal base motions comprising 12 synthetic ground accelerograms compatible with the NBC Uniform Hazard Spectra (UHS) for Montréal (Halchuk 2001), corresponding to a probability of exceedance of 2% in 50 years. The records are independently applied to both principal horizontal directions (longitudinal and transverse directions) of each building as prescribed in the NBC 2005 (section 4.1.8.8) (National Research Council Canada 2005). The linear time-history seismic analysis has been carried out using SAP2000 (Computers and Structures 2009). Then, selecting two floors in each block (top floor #7 and middle floor #3), floor response spectra and inter-storey drift curves were developed for each record.

5. RESULTS AND DISCUSSION

Table 5.1 reports the experimental results extracted by enhanced frequency domain decomposition of the AVM records for the three lowest frequency modes of each tested building.

Tables 5.2 and 5.3 compare the fundamental sway-mode period of the two blocks according to the empirical formula recommended in NBC 2010 for concrete moment-resisting frames and the fundamental period extracted from AVM records. The results show that the fundamental period extracted from AVM records is roughly half the period calculated based on the NBC formula. On the one hand, it is recognized that AVM are conducted at very low strain levels, very far from the slightly damaged state that is expected during a design level earthquake, while code formulas represent an ultimate limit state of the building responding to a design-level maximum considered earthquake. On the other hand, operational conditions include the real reactive mass of the structure as well as the presence of non-structural components (in particular the effect of stiff partitions and infilled walls), and the effect of the foundations and soil at the site.

Table 5.1. AVM results (Blocks #7 & #8)

Mode shape	1st transverse mode		1st longitudinal mode		1st torsional mode	
Block #8						
Models	Period (s)	Frequency (Hz)	Period (s)	Frequency (Hz)	Period (s)	Frequency (Hz)
ARTeMIS-EFDD-Aug 2010	0.53	1.90	0.38	2.67	0.40	2.48
Block #7						
Mode shape	1st transverse mode		1st longitudinal mode		1st torsional mode	
Models	Period (s)	Frequency (Hz)	Period (s)	Frequency (Hz)	Period (s)	Frequency (Hz)
ARTeMIS-EFDD-Sep 2010	0.54	1.86	0.49	2.05	0.33	3.06
ARTeMIS-EFDD-July 2011	0.55	1.83	0.50	2.00	0.35	2.88

Table 5.2. Fundamental period calculation based on NBC 2010

Empirical period- NBC 2010	Building height h_n (m)	Fundamental period T_a (s)	Fundamental frequency f (Hz)
$T_a=0.075(h_n)^{3/4}$	36.11	1.10	0.91

Table 5.3. Comparison between AVM results and NBC 2010

	Models	Fundamental Period (s)		Models	Fundamental Period (s)
Block # 8	NBC 2010	1.10	**Block # 7**	NBC 2010	1.10
	ARTeMIS-EFDD-Aug 2010	0.53		ARTeMIS-EFDD-Sep 2010	0.54
	Difference (%)	109.8%		Difference (%)	105.5%

Table 5.4 shows the results of different finite element models and also the AVM results for Block # 8: it is seen that adding the *terra cotta* infill walls to the bare-frame model of Block #8 increases the natural frequencies of the building by 70%-77% when comparing the bare-frame model with AVM, and by 41%-78% when comparing the bare-frame model with the full-frame models. This increase in natural frequencies is due to the increased lateral stiffness of the building contributed by the masonry infill walls. Considering the results, the continuum model shows the closest frequencies to the AVM results with a difference less than 12%, which is deemed acceptable. Therefore, it can be concluded that in this particular case-study the best technique among the adopted methods for modeling the infill walls is the continuum model with plane stress panel elements.

Table 5.4. Numerical and experimental results - Block # 8

Mode shape	1st transverse mode		1st longitudinal mode		1st torsional mode	
Models	Period (s)	Frequency (Hz)	Period (s)	Frequency (Hz)	Period (s)	Frequency (Hz)
Bare-frame model	1.76	0.57	1.56	0.64	1.53	0.65
Full-frame models						
Continuum model	0.60	1.66	0.35	2.88	0.41	2.43
Stafford Smith strut model	0.91	1.10	0.60	1.68	0.69	1.45
Durrani strut model	0.90	1.11	0.60	1.66	0.69	1.45
FEMA-356 strut model	1.04	0.97	0.76	1.32	0.83	1.21
Experimental results (AVM)						
ARTeMIS-EFDD-Aug 2010	0.53	1.90	0.38	2.67	0.40	2.48

Considering the results of Block # 7 summarized in Table 5.5, the natural frequencies are increased by 1%-27% after adding the infill walls, which is less than the increase observed in Block # 8. The main explanation is that when disregarding the infill walls, Block #7 is much stiffer than Block #8 owing to

the presence of the concrete shear wall and the structural connection with Block #9. As a result, the infill walls do not affect the dynamic properties of Block #7 as much as Block #8.

Table 5.5. Numerical and experimental results - Block # 7

Mode shape	1st transverse mode		1st longitudinal mode		1st torsional mode	
Models	Period (s)	Frequency (Hz)	Period (s)	Frequency (Hz)	Period (s)	Frequency (Hz)
Bare-frame model	0.64	1.56	0.31	3.19	0.17	5.79
Full-frame models						
Continuum model	0.47	2.14	0.25	4.00	0.18	5.63
Stafford Smith strut model	0.58	1.72	0.31	3.21	0.19	5.32
Durrani strut model	0.58	1.74	0.30	3.35	0.18	5.48
FEMA-356 strut model	0.61	1.64	0.31	3.22	0.18	5.43
Experimental results (AVM)						
ARTeMIS-EFDD-Sep 2010	0.54	1.86	0.49	2.05	0.33	3.06
ARTeMIS-EFDD-July 2011	0.55	1.83	0.50	2.00	0.35	2.88

Table 5.6. Natural periods and frequencies of bare-frame and continuum models

Models	Mode Shapes	Block # 8				Block # 7			
		First mode		Second mode		First mode		Second mode	
		Period (s)	Frequency (Hz)	Period (s)	Frequency (Hz)	Period (s)	Frequency (Hz)	Period (s)	Frequency (Hz)
Bare-frame model	X direction	1.57	0.64	0.58	1.73	0.31	3.19	0.26	3.84
	Y direction	1.76	0.57	0.66	1.51	0.61	1.63	0.23	4.36
	Torsion	1.53	0.65	0.56	1.8	-----	-----	-----	-----
Continuum model	X direction	0.35	2.88	-----	-----	0.25	4	-----	-----
	Y direction	0.6	1.66	0.18	5.44	0.47	2.14	-----	-----
	Torsion	0.41	2.43	-----	-----	0.18	5.63	-----	-----

Figures 5.1.a and c illustrate the FRS curves in terms of pseudo-acceleration, developed for Block # 8 at the 7th floor separately in each horizontal direction (i.e. X and Y). It can be seen that the presence of masonry infill walls, resulting in a significant increase in the calculated fundamental frequencies of the building, causes the NSCs mounted on floors to experience much larger accelerations than if infill walls are not considered, which may become critical for acceleration sensitive NSCs. However, for those NSCs which are sensitive to the inter-storey drift, the presence of masonry infill walls contributes to reduce the demand in drift, as seen in Figures 5.1.b and d and Table 5.7.

In general, similar conclusions can be made for Block #7. The increase in acceleration and decrease in inter-storey drift caused by the presence of masonry infill walls is observed in Figures 5.1.e and g, 5.1.f and h, and Table 5.7, respectively. However, in Block #7 the difference between bare-frame and continuum models is less than for Block #8, as Block #7 benefits from the presence seismic retrofit, i.e. the added shear wall and the structural connection to Block #9.

Looking at the FRS in terms of pseudo-acceleration and displacement curves, a number of peaks are observed in each horizontal direction (X and Y). Theses peaks are directly related to the natural frequencies of each model corresponding to each direction (Table 5.6). It is expected that the response of the main building (primary structure) at each floor shows the peaks at natural frequencies due to resonance. Then, the acceleration response of all floors is considered as the base acceleration for NSCs (Subsystem) to develop the FRS. As the floor response has higher energy content at natural frequencies of the primary structure, the FRS will also have peaks at the same frequencies.
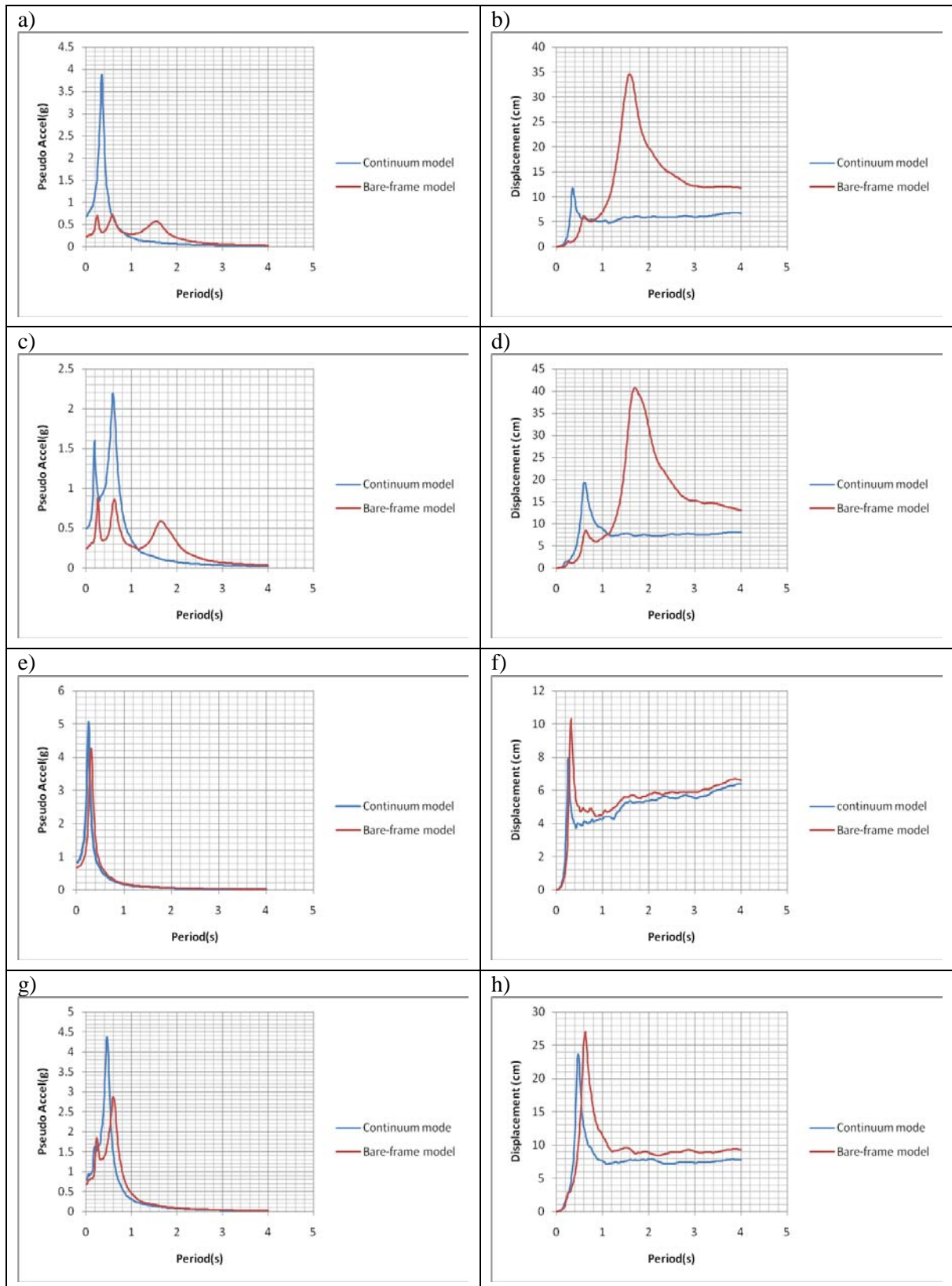
Figure 5.1. Averaged floor response spectra – 7th floor: a) Block # 8 - X-direction-Pseudo acceleration; b) Block # 8 - X-direction-Displacement; c) Block #8- Y-direction-Pseudo acceleration; d) Block #8- Y-direction-Displacement; e) Block #7- X-direction-Pseudo acceleration; f) Block #7- X-direction-Displacement; g) Block #7- Y-direction-Pseudo acceleration; h) Block #7- Y-direction-Displacement.

Table 5.7. Maximum Inter-storey drift – Blocks # 7 and #8

	Block #8 Maximum Inter-storey drift (%)				**Block #7** Maximum Inter-storey drift (%)			
	7th floor- X direction		7th floor- Y direction		7th floor- X direction		7th floor- Y direction	
MODEL	Bare-frame model	Continuum model	Bare-frame model	Continuum model	Bare-frame model	Continuum model	Bare-frame model	Continuum model
Records	(%)	(%)	(%)	(%)	(%)	(%)	(%)	(%)
E60301	0.30	0.02	0.50	0.09	0.15	0.01	0.17	0.07
E60302	0.25	0.02	0.38	0.07	0.15	0.01	0.12	0.08
E60501	0.34	0.03	0.36	0.08	0.13	0.01	0.14	0.07
E60502	0.29	0.02	0.34	0.08	0.14	0.01	0.10	0.07
E70301	0.22	0.01	0.32	0.08	0.13	0.01	0.12	0.10
E70302	0.29	0.02	0.37	0.12	0.12	0.01	0.18	0.08
E70501	0.28	0.02	0.39	0.10	0.15	0.01	0.13	0.06
E70502	0.20	0.02	0.35	0.08	0.12	0.01	0.13	0.0
E70701	0.25	0.02	0.36	0.10	0.13	0.01	0.17	0.07
E70702	0.30	0.02	0.45	0.45	0.16	0.01	0.16	0.07
E701001	0.28	0.02	0.43	0.07	0.14	0.01	0.12	0.09
E701002	0.38	0.02	2.84	0.15	0.13	0.01	0.23	0.08
Average	0.28	0.02	0.59	0.12	0.14	0.01	0.15	0.08

6. CONCLUSIONS

The main scope of this study was to examine the effects of seismic retrofits and the presence of *terra cotta* infill walls on the dynamic characteristics of two similar hospital buildings, and their influence on the seismic performance of floor-mounted non-structural components.

The results of ambient vibration tests and finite element models showed that considering masonry infill walls in modeling affect the dynamic properties of the structures considerably: decreasing the fundamental period of Blocks #8 and #7 by nearly 200% and 40%, respectively in this particular case study.

The floor response spectra and inter-storey drift curves were derived for two selected floors of each block (floor levels 3 and 7) considering a series of 12 earthquake records. These results showed that the global lateral stiffening of the buildings due to the presence of *terra cotta* infill walls has two main effects: 1- Acceleration-sensitive components attached to upper floors are subjected to the higher acceleration when the building is stiffer and 2- Displacement-sensitive components are experiencing lower drifts, which is beneficial to their seismic performance.

ACKNOWLEDGMENT

REFERENCES

Amrhein, J.E. 1998. Reinforced masonry engineering handbook: clay and concrete masonry. CRC Press.

Asgarian, A. 2012. "Impact of seismic retrofit and presence of terra cotta masonry walls on the dynamic properties of a hospital building in Montreal, Canada." Master of Engineering, Department of Civil Engineering and Applied Mechanics, McGill Univeristy.

CSA Canadian Standards Association. 2006. "Seismic risk reduction of operational and functional

components (OFCs) of buildings, CAN/CSA-S832-06(R11)."

Chartrand, V. 2009 "Seismic Retrofitting of the Ste-Justine Hospital in Montreal." Master of Engineering, Department of Civil and Environmental Engineering, Massachusetts Institute of Technology.

ACI American Concrete Institute, Joint ACI/ASCE/TMS Committee . 2005. Building code requirements for masonry structures (ACI 530-05/ASCE 5-05/TMS 402-05); Specification for masonry structures (ACI 530.1-05/ASCE 6-05/TMS 602-05); Commentary on building code requirements for masonry structures (ACI 530-05/ASCE 5-05/TMS 402-05); Commentary on specification for masonry structures (ACI 530.1-05/ASCE 6-05/TMS 602-05). Masonry Society. 2005. Specification For Masonry Structures (ASCI 530.1/ASCE 6-92/TMS 602-902). American Concrete Institute International.

SAP 2000-advanced 14.0.0. Computers & Structures, Inc. http://www.csiberkeley.com/sap2000

Durrani, A.J., YH Luo, and D.P. Abrams. 1994. Seismic retrofit of flat-slab buildings with masonry infills. Technical Report NCEER Workshop on Seismic Response of Masonry Infills, San Francisco, California, 4-5 Feb 1994, 1-8.

El-Dakhakhni, W.W. 2002. "Experimental and analytical seismic evaluation of concrete masonry-infilled steel frames retrofitted using GFRP laminates." PhD Thesis, Department of Civil, Architectural & Environmental Engineering, Drexel University.

El-Dakhakhni, W.W., M. Elgaaly, and A.A. Hamid. 2003. Three-strut model for concrete masonry-infilled steel frames. ASCE Journal of Structural Engineering, 129 (2): 177-185.

El-Dakhakhni, W.W. 2000. "Non-linear finite element modeling of concrete masonry-infilled steel frames". 1st ed. Drexel University.

FEMA, and ASCE. 2000. "FEMA-356, Prestandard and commentary for the seismic rehabilitation of buildings."

Gilles, D. 2011. "In situ dynamic characteristics of reinforced concrete shear wall buildings." PhD thesis, Department of Civil Engineering and Applied Mechanics,   McGill University.

Halchuk, S., and J. Adams. 2004. "Fourth Generation Seismic Hazard Maps for Canada." 13th World Conference on Earthquake Engineering, Vancouver, B.C., Canada.

Hendry, A.W. 1981. Structural brickwork. Halsted Press.

Holmes, M. 1961. Steel frames with brickwork and concrete infilling. Proceedings of the Institution of Civil Engineers 19: 473 –478.

Luo, Y. 1995. "Evaluation, Modeling, and Retrofit of Flat-Slab Buildings Subjected to Seismic Loading." PhD thesis, Department of Civil and Environmental Engineering, Rice University.

Mainstone, R.J., and Building Research Station. 1974. "On Stiffnesses and Strengths of Infilled Frames". Building Research Station. http://books.google.com/books?id=iQJEAQAAIAAJI

Mohyeddin-Kermani, A., H.M. Goldsworthy, and E. Gad. 2008. "A Review of the Seismic Behaviour of RC Frames with Masonry Infill." Australian Earthquake Engineering Society Conference(AEES 2008), Ballarat, Victoria, Australia.

National Research Council Canada, Institute for Research in Construction. 2005&2010. "National Building Code of Canada (NBC)."

Polyakov, S. V. 1960. On the Interaction between Masonry Filler Walls and Enclosing Frame when Loaded in the Plane of the Wall. Earthquake Engineering, 36-42.

Schott, J.R. 2005. Matrix analysis for statistics. 2nd ed.: Wiley-Interscience.

Shing, P.B., and A.B. Mehrabi. 2002. Behaviour and analysis of masonry-infilled frames. Progress in Structural Engineering and Materials, 4 (3): 320-331.

Structural Vibration Solutions A/S. (2009a). "ARTeMIS Extractor Handy (Version 4.2) [Software]." http://www.svibs.com.